Journal Pre-proof



Groundwater remediation using Magnesium–Aluminum alloys and *in situ* layered doubled hydroxides

Jingqi Zhang, Hanjun Hu, Jingbo Chao, Yang Tang, Pingyu Wan, Qipeng Yuan, Adrian C. Fisher, Frederic Coulon, Qing Hu, Xiao Jin Yang

PII: S0013-9351(21)01542-5

DOI: https://doi.org/10.1016/j.envres.2021.112241

Reference: YENRS 112241

To appear in: *Environmental Research*

Received Date: 13 November 2020

Revised Date: 8 October 2021

Accepted Date: 16 October 2021

Please cite this article as: Zhang, J., Hu, H., Chao, J., Tang, Y., Wan, P., Yuan, Q., Fisher, A.C., Coulon, F., Hu, Q., Yang, X.J., Groundwater remediation using Magnesium–Aluminum alloys and *in situ* layered doubled hydroxides, *Environmental Research* (2021), doi: https://doi.org/10.1016/j.envres.2021.112241.

This is a PDF file of an article that has undergone enhancements after acceptance, such as the addition of a cover page and metadata, and formatting for readability, but it is not yet the definitive version of record. This version will undergo additional copyediting, typesetting and review before it is published in its final form, but we are providing this version to give early visibility of the article. Please note that, during the production process, errors may be discovered which could affect the content, and all legal disclaimers that apply to the journal pertain.

© 2021 Published by Elsevier Inc.

Environmental Research, Volume 204, Part C, March 2022, Article number 112241
DOI:10.1016/j.envres.2021.112241
Journal Pre-proof

CRediT author statement

Jingqi Zhang: Methodology, Validation, Formal analysis, Visualization, Writing - Original Draft. **Hanjun Hu:** Methodology, Validation, Visualization. **Jingbo Chao:** Resources, Funding acquisition. **Yang Tang:** Software, Methodology. **Pingyu Wan:** Investigation, Writing - Review & Editing, Project administration. **Qipeng Yuan:** Writing - Review & Editing. **Adrian C. Fisher:** Writing - Review & Editing. **Frederic Coulon:** Project administration, Writing - Review & Editing. **Qing Hu:** Project administration, Funding acquisition. **Xiao J. Yang:** Conceptualization, Methodology, Resources, Writing - Review & Editing, Visualization, Supervision.

Journal Pre-proof

Abstract:
In situ remediation of groundwater by zerovalent iron (ZVI)-based technology faces the problems of rapid passivation, fast agglomeration, limited range of pollutants and secondary contamination. Here a new concept of Magnesium–Aluminum (Mg–Al) alloys and*in situ*layered double hydroxides on is proposed for the degradation and removal of a wide variety of inorganic and organic pollutants from groundwater. The Mg–Al alloy provides the electrons for the chemical reduction and/or the degradation of pollutants while released Mg^{2+}, $Al^{3+}$and OH^{-}ions react to generate*in situ*LDH precipitates, incorporating other divalent and trivalent metals and oxyanions pollutants and further adsorbing the micropollutants. The Mg–Al alloy outperforms ZVI for treating acidic, synthetic groundwater samples contaminated by complex chemical mixtures of heavy metals (Cd^{2+}, Cr^{6+}, Cu^{2+}, $Ni^{2+}$and Zn^{2+}), nitrate, AsO_3^{3-}, methyl blue, trichloroacetic acid and glyphosate. Specifically, the Mg–Al alloy achieves removal efficiency ≥99.7% for these multiple pollutants at concentrations ranging between 10 and 50mgL^{-1}without producing any secondary contaminants. In contrast, ZVI removal efficiency did not exceed 90% and secondary contamination up to 220mgL^{-1}Fe was observed. Overall, this study provides a new alternative approach to develop efficient, cost-effective and green remediation for water and groundwater.

Keywords
Groundwater remediation; Chemical degradation; Mg–Al alloy; In situ layered double hydroxides

Published by Elsevier. This is the Author Accepted Manuscript issued with: Creative Commons Attribution Non-Commercial No Derivatives License (CC:BY:NC:ND 4.0).
The final published version (version of record) is available online at DOI:.10.1016/j.envres.2021.112241 Please refer to any applicable publisher terms of use.

1. Introduction

Groundwater pollution is a worldwide problem (Schwarzenbach et al. 2006; Shannon et al. 2008) posing a significant challenge for the remediation sector, especially in developing and implementing efficient, green and sustainable remediation treatments (Chih-Ming et al. 2020; Schwarzenbach et al. 2006; Shannon et al. 2008). While *in situ* treatment technologies using various materials such as carbon materials, layered doubled hydroxides (LDH), zeolites, TiO_2 and metal organic frameworks, are seen as the most cost-effective for groundwater remediation, their performance and effectiveness can vary greatly with site specific conditions and be impaired by other substances in groundwater (Ali et al. 2018; Saleh 2020a; b; c; Saleh and Ali 2018; Yang et al. 2016; Zubair et al. 2017). For example, active carbon (AC) is a classic carbon adsorbent for water treatment but it is not highly effective for the removal of inorganic pollutants and heavy metals, particularly in acidic waters (Jeirani et al. 2017; Tran et al. 2017). Similarly, LDH, a class of anionic clays with a highly tuneable brucite structure, has attracted great attention as an emerging biocompatible material in a wide range of applications, including environmental and water remediation (Boclair and Braterman 1999; Ma et al. 2017; Theiss et al. 2014; Zubair et al. 2017). However, the unique structure of LDH collapses when exposed to highly acidic water environment and therefore rendering it unsuitable for remediation purpose. Further to this, adsorption-based methods suffer a high risk of re-contamination. In this context, chemical oxidation-reduction/degradation using zerovalent iron (ZVI) and nanoscale zerovalent iron (nZVI) is of advantages for *in situ* groundwater remediation (Fu et al. 2014; Guan et al. 2015; Li et al. 2019). However, ZVI and nZVI suffer poor adsorption, rapid passivation, fast agglomeration and sedimentation, and secondary contamination (Bae et al. 2018; Chih-Ming et al. 2020; Cohen and Weisbrod 2018; Guan et al. 2015). Furthermore, ZVI and nZVI are inadequate for some heavy metals such as Cd^{2+}, Ni^{2+} and refractory organic contaminants and toxic oxygenated anions (Guan et al. 2015; Li et al. 2019). To overcome these issues, bi-metals (Fe/Al, Fe/Ni, Fe/Cu, Pd/Al) and Al alloys (Al-Fe, Al-Ni, Al-Cu) have been investigated (Bao et al. 2017; Fu et al. 2015; Tosco et al. 2014; Xu et al. 2018; Zhang et al. 2019). The major problem associated with these metal-based materials is secondary contamination by the release of metal ions (Al, Fe, Ni, Cu, etc.) (Bao et al. 2017; Fu et al. 2015; Guan et al. 2015). To date there is still a pressing need for developing new materials that can overcome the inherent problems encountered with ZVI and nZVI (Guan et al. 2015; Li et al. 2019).

Recent studies have been looking into the development of nanocomposite materials by combining nZVI

with AC or LDH to take the advantages of chemical degradation and adsorption (Cohen and Weisbrod 2018; Shukla et al. 2018; Wang et al. 2019; Xu and Huang 2019; Yu et al. 2019). While nZVI-AC and nZVI-LDH composite materials avoid fast aggregation and agglomeration, the reactivity of nZVI and the adsorption capacity of AC and LDH in the nZVI-AC and nZVI-LDH nanocomposites have been shown to be easily impaired by the presence of other contaminants in groundwater (Wang et al. 2019; Xu and Huang 2019; Yu et al. 2019; Zhou et al. 2020). Furthermore, the complicated preparation procedures, high cost, limited lifespan and ecotoxicity of these composite nanomaterials are major limitations for their field applications (Saleh 2020b; Wang et al. 2019; Nguyen et al. 2018).

In this study, a new concept of Mg-Al alloy and its derived *in situ* LDH is proposed for groundwater remediation using heavy metals, typical anions and organics as model pollutants (Fig. 1). Specifically, Mg-Al alloy reacts with water (via hydrolysis) and the model pollutants Cu^{2+}, $Cr_2O_7^{2-}$, trichloroacetic acid, etc. (via chemical reduction) to produce Mg^{2+}, Al^{3+}, Cu^0, Cr^{3+}, OH^- and Cl^-. Then, Mg^{2+}, Al^{3+}, other divalent and trivalent metal ions (Ni^{2+}, Zn^{2+}, Cd^{2+}, Cr^{3+}), OH^- and anions (Cl^-, CO_3^{2-}, SO_4^{2-}, AsO_3^{3-} and $Cr_2O_7^{2-}$) react to generate *in situ* hybrid LDH, which further adsorbs organic pollutants and other potential secondary pollutants. Mg-Al alloy is relatively low in density and of no magnetic while LDH is biocompatible and therefore, Mg-Al alloy/*in situ* LDH is expected to extend the range of pollutants and overcome the inherit problems of poor adsorption, rapid aggregation and secondary contamination in the ZVI-based remediation technology.

2. Materials and methods

2.1 Reagents and samples

$Ni(NO_3)_2{\cdot}6H_2O$ (99.7%) and $Cu(NO_3)_2{\cdot}3H_2O$ (99.7%) were purchased from Tianjin Fuchen Chemical Reagent Factory (China). $Zn(NO_3)_2{\cdot}6H_2O$ (99.7%) and $AlCl_3{\cdot}6H_2O$ (99.7%) were obtained from Xilong Chemical (China). $Cd(NO_3)_2{\cdot}3H_2O$ (99.7%), $MgCl_2{\cdot}6H_2O$ (99.7%), $NaNO_3$ (99.8%), $NaNO_2$ (99.8%), NH_4Cl (99.8%), salicylic acid (99.7%), potassium sodium tartrate (99.7%), sodium nitroprusside (99.7%), sodium hypochlorite (99.7%), HCl (99.7%) and NaOH (99.7%) were purchased from Beijing Chemical Works (China). $K_2Cr_2O_7$ (99.7%) and Mg metal powders (>240 mesh) were purchased from Tianjin Guangfu Fine Chemical Research Institute (China). Powders of Al metal (>325 mesh) and ZVI (100-120 mesh) were purchased from Tianjin Fuchen Chemical Reagent Factory. Activated carbon (>200 mesh) and

Mg/Al layered doubled hydroxide were purchased from Aladdin and Heowns, respectively. Stock multiple element standard solutions (GBW(E) 081532-081535) for ICP-OES calibration were obtained from National Institute of Metrology of China. Glyphosate (>99.5%), trichloroacetic acid (>99%), 2,4,6-trichlorophenol (>98%) and methyl blue (>98%) were purchased from Aladdin. Aqueous solutions of pollutants were prepared by dissolving heavy metals nitrates and organic compounds in ultrapure water (18.2 MΩ.cm, Millipore, USA) and adjusting to required pH with dilute HCl (1 M and 5 M) and NaOH (1 M) solutions. Groundwater samples were taken from 90-m underground in the northwest suburb of Beijing. Ultrapure water was used for preparation of solutions and contaminated water.

2.2 Materials and instrumentation

Mg-Al alloys were prepared by melting pure Mg (>99.9%) and Al (>99.9%) ingots (mass ratio 60:40) using MgO crucible in a vacuum electric furnace (SGM.VB6/16, Sigma Furnace Industry, China) at a vacuum pressure of < 5 Pa. The temperature of the furnace was increased from room temperature to 800 □ at a rate of 7 □/min and was maintained for 30 min. The furnace was then cooled to room temperature and the Mg-Al alloy ingot was crushed into >200 mesh powders.

Materials were characterized by X-ray diffraction (Ultima IV, XRD-6000, Japan) at 40 kV/40 mA with Cu Ka radiation (l = 1.5406 Å) with a scan rate of 5° min^{-1} in the 2θ range of 5–90° and scanning electron microscope (Hitachi, S4700, Japan). Particle size distribution was measured by dynamic light scattering (Malvern, Nano ZS90, U.K.). BET specific surface areas were measured from the N_2 adsorption and desorption isotherms at 77 K collected from a Autosorb-IQ gas adsorption analyzer (Quantachrome, U.S.A.).

The concentration of heavy metals, Al, Mg and Fe was determined by ICP-OES (Thermo, iCAP 6000, U.S.A.). The concentration of nitrate, trichloroacetic acid and glyphosate were measured by ion chromatography (Dionex, ICS-900, U.S.A.) using an IonPac AS19 (4*250 mm) analytical column and IonPac AG19 (2*50 mm) guard column with 35 mM NaOH at a flow rate of 0.5 mL min^{-1}. The retention time of nitrate, trichloroacetic acid and glyphosate was 10.1, 12.4 and 13.5 min, respectively. Methyl blue was determined by UV-vis photometer (TU-1900, Persee, China) at a wavelength of 600 nm. The pH meter (Mettler Toledo, FE 20, Switzerland) was used to measure pH of the solution.

2.3 Removal experiments

Fig. S1 provides an overview of the experimental apparatus used. Three g of alloy materials were added into the 500 mL glass bottle with a two-outlet tube cap. One outlet tube was inserted into a bottom-up placed

measuring cylinder filled with water for H_2 collection. After air tight test by injection syringe with measurements (Fig. S1a), 300 mL aqueous solution containing 25 mg L^{-1} heavy metals and 40 mg L^{-1} NO_3^- were rapidly pumped into the bottle through the other outlet tube (Fig. S1b). The solution was stirred with a magnetic bar at 350 rpm (Fig. S1c, IKA, RO10, Germany). The room temperature was set at 22±2 □. The pH of the solution was adjusted to pH 2 with diluted HCl (0.1 and 1 M) and NaOH (0.1 and 1 M) prior to loading to the reactor unless otherwise specified. Samples of 3 mL were drawn through the other outlet tube at a certain time interval and filtered with 0.22 μm nylon membrane filters (Jinteng, China). Part of the filtered samples were acidified to 2% HNO_3 prior to ICP-OES for metal analysis and part of the samples were analyzed for organic pollutants after appropriate dilution (see section 2.2). After reaction, the solid materials and/or precipitates were filtered with filter paper, washed with deionized water several times and dried in a vacuum oven (-0.9 MPa) at 60 □ for 12 h.

3. Results and discussion

3.1 *In situ* formation of LDH by Mg-Al alloy hydrolysis

The most important parameters for the co-precipitation process of Mg/Al-LDH are pH, Mg^{2+} and Al^{3+}concentrations and their ratio, the reaction temperature and time (Bukhtiyarova 2019; Theiss et al. 2016). The dissolution rate of Mg and Al from Mg-Al alloy hydrolysis is determined by the pH of the solution, the composition and structure of the alloy and the temperature (Guo et al. 2018). In this study, the *in situ* formation of LDH from the Mg-Al alloy with a mass ratio of 64/40 was investigated. For comparison, metallic Mg powders in $AlCl_3$ solution (Mg+$AlCl_3$), metallic Al powders in $MgCl_2$ solution (Al+$MgCl_2$), and mixtures of metallic Mg and Al powders (Mg+Al) were also investigated (Fig. 2). The Mg-Al alloy is dominated by the phase of intermetallic $Mg_{17}Al_{12}$, a cubic crystal as identified by the characteristic diffraction peaks of planes (330), (332) and (721) at 2θ of 36.8°, 40.2° and 65.2°, respectively (JCPDS Card No. 01-1128) (Fig. 2a). The hydrolysis product of the Mg-Al alloy is LDH, a hexagonal crystal as identified by the typical diffraction peaks of planes (003), (006) and (012) at 2θ of 11.6°, 23.4° and 34.9°, respectively (JCPDS Card No. 89-0460) (Fig. 2b). By contrast, the hydrolysis product of Mg+$AlCl_3$ are mixtures of LDH and $Mg(OH)_2$ while no LDH is observed in the hydrolysis products of Al+$MgCl_2$ and Mg+Al. The SEM characterization (Fig. 2c, d) shows that the hydrolysis product of the Mg-Al alloy displays a typical flower-like structure of LDH. In a recent study, the composition and the BET surface area of the LDH

obtained by the hydrolysis of Mg-Al alloys were determined to be $[Mg_{18}Al_7(OH)_{50}][Cl_3(CO_3)_{25}H_2O]$ and 37-55 m^2/g, respectively (Zheng et al. 2021).

The Mg^{2+} and Al^{3+} concentrations, the pH of solution and hydrogen generation during the hydrolysis are shown in Fig. 3. For Mg-Al alloy (Fig. 3a, b), Mg^{2+} and Al^{3+} concentrations increase rapidly to 59.9 and 9.4 mg L^{-1} within 2 h and then decrease slowly to 9.3 and 5.2 mg L^{-1}, respectively at the end of the reaction process (Fig. 3a). The pH of solution increases sharply to pH 8.7 within 0.5 h from initial pH 2 and then remains almost unchanged (Fig. 3b). For Mg+$AlCl_3$ (Fig. 3c, d), Mg^{2+} concentration increases to 180 mg L^{-1} within 1 h and then remains almost constant in the following period of 23 h while Al^{3+} concentration decreases from initial value of 100 mg L^{-1} to 5.37 mg L^{-1} in 0.5 h (Fig. 3c). The pH profile of Mg+$AlCl_3$ (Fig. 3d) is similar with that of Mg-Al alloy (Fig. 3b) but hydrogen generation is different (Fig. 3b, d). The hydrolysis reaction is instantaneous in both systems and the difference is that hydrogen generation reaches 130 mL in the beginning 3 h and then stops in the Mg-Al alloy system while it reaches 83 mL in the beginning and then slowly increases to 200 mL by the end of experiment. For comparison, Mg^{2+} concentration, pH variation and hydrogen generation of the hydrolysis of Mg metallic powders are shown in Fig. S2. The above observation indicates that the Mg-Al alloy is active right at the onset of the process and up to 5 h of reaction and then the surface is passivated while Mg metal is active to generate hydrogen during the whole period of the experiment. The passivation of Mg-Al alloy surface is likely caused by the formation of LDH (refer to Fig. 2b) as LDH coatings have proved to improve the corrosion resistance of Mg meal and Mg alloys (Guo et al. 2018). It is worthy to mention that the passivation does not occur to Mg metal although LDH formation is also observed in the Mg+$AlCl_3$ system (Fig. 2b). Probably, the mechanism of *in situ* LDH formation is different in these two systems and indeed, a larger amount of $Mg(OH)_2$ is produced in the Mg+$AlCl_3$ system (Fig. 2b).

In the Al+$MgCl_2$ system (Fig. 3e, f), Mg^{2+} concentration does not change relative to the added concentrations during the whole period of the experiment. Al^{3+} ion is not observed in the initial period of 3 h but its concentration increases rapidly afterwards. A small amount of hydrogen is produced at the onset but the reaction terminates immediately. The solution pH increases from 2.0 to 4.0 in 9 h and then stabilizes at pH 4.2. Therefore, Al^{3+} concentration is the result of the dissolution of Al oxide layer on the surface of Al metal particles while the pH stabilization at pH 4.2 indicates re-passivation of the Al metal surface. The value of pH 4.2 is far too low to form LDH or $Mg(OH)_2$ precipitates. Consequently, Mg^{2+} is not consumed

and LDH is not generated.

An interesting phenomenon is observed in the Mg+Al system where the Mg^{2+} and Al^{3+} concentration ratio and the pH value fulfil the requirement of LDH formation (Fig. 3g, h) while LDH is not produced (Fig. 2b). The hydrolysis reaction follows a biphasic process. Within the first 9 hours, the reaction dominates on Mg metal particles, consuming H^+ while producing Mg^{2+}, OH^- and H_2. During that period the Al oxides on the surface of Al metal particles dissolve and the Mg metal surface is gradually passivated. Then, the hydrolysis mainly occurs on Al metal, resulting in a rapid increase of H_2 generation.

It was reported that the nucleation of Mg/Al-LDH is critical in the co-precipitation method for the preparation of LDH crystallites (Bukhtiyarova 2019; Theiss et al. 2016). The Mg-Al alloy employed in this study is a component of $Mg_{17}Al_{12}$, the hydrolysis of which releases Mg^{2+} and Al^{3+} simultaneously and therefore, Mg^{2+}/Al^{3+} ratio is relatively constant. By contrast, the hydrolysis of Mg+Al is in a biphasic process in which Mg^{2+}/Al^{3+} ratio varies during the hydrolysis. Therefore, it is probably more difficult to generate the nucleation seed of Mg/Al-LDH in the Mg+Al system than in the Mg-Al alloy system.

3.2 Removal of heavy metals and nitrate

Fig. 4 shows the performance of the above 4 systems for simultaneously removing Cd^{2+}, $Cr_2O_7^{2-}$, Cu^{2+}, Ni^{2+}, Zn^{2+} (25 mg L^{-1} each) and NO_3^- (40 mg L^{-1}). For comparison, Mg metal powders were also investigated. Clearly, Mg-Al alloy and Mg+$AlCl_3$ performed much better than the other three systems (>85% removal within 2 hours) (Fig. 4a, c). Overall, the removal efficiencies of the heavy metals using either Mg+$AlCl_3$ or Mg-Al alloy are similar and their reaction rates both follow a pseudo-first-order reaction with constant rate of 5.3 h^{-1}, 4.0 h^{-1}, 4.0 h^{-1}, 3.4 h^{-1} and 1.9 h^{-1} ($R^2 > 0.88$) for Cu, Zn, Ni, Cr and Cd, respectively. No contaminants are removed by Al+$MgCl_2$ (Fig. 4e) and lower rates of heavy metals removal are observed in the Mg+Al system than in the Mg system (Fig. 4g, i). Of the five systems, Mg-Al alloy shows the highest removal rate for the heavy metals and nitrate. Interestingly, Mg-Al alloy removes 73% of NO_3^- in 9 h (Fig. 4a) while Mg+$AlCl_3$ removes only 12% (Fig. 4c) and Mg+Al and Mg alone were ineffective (Fig. 4g, i).

In general, the removal of heavy metals by active zerovalent metals (e.g., Al and Fe) is via a combination of chemical reduction ($Cu^{2+} \rightarrow Cu^0$) with co-precipitation of metal hydroxides (Fu et al. 2014; Nidheesh et al. 2018) while nitrate removal by ZVI is dominated by chemical reduction (Fu et al. 2014). The pH and concentrations of Mg^{2+} and Al^{3+} were measured (see the right panel of Fig. 4) and the materials after the

175 removal process were characterized by XRD and SEM (Fig. 5) to understand the process. In this study, the
176 removal of the heavy metals by Mg-Al alloy is likely a combined effect of chemical reduction (e.g., $Cu^{2+}\rightarrow$
177 Cu^{0}, $Cr^{6+}\rightarrow Cr^{3+}$), hydroxide co-precipitation and *in situ* formation of hybrid LDH (such as $Mg/Al/Cr^{III}$,
178 Mg/Cd/Al, Mg/Zn/Al, $Mg/Zn/Cr^{III}$). LDH is clearly observed in the Mg-Al alloy and Mg+$AlCl_3$ systems
179 (Fig. 5a, b) whereas LDH is not produced in the systems of Al+$MgCl_2$, Mg+Al and Mg metal alone (Fig.
180 5c, d, e). LDH shows high capacity for the adsorption of a wide variety of pollutants from water (Zubair et
181 al. 2017) and therefore, the *in situ* formation of LDH enhances the removal rates. The highest removal rates
182 of the pollutants by Mg-Al alloy are attributed to its fastest rate of Mg and Al dissolution (the effect of
183 galvanic corrosion between Al and Mg) and the largest amount of LDH produced. Neither the Al+$MgCl_2$
184 nor the Mg+Al systems produce LDH (Fig. 5c, d) as the dissolution of metallic Al powders does not occur
185 (Fig. 4f, g) due to the protection of the dense alumina layer on the surface of metallic Al (Nidheesh et al.
186 2018).

187 The concentration of NO_2^- and NH_4^+ in the Mg-Al alloy system at the end of experiment were ≥68% of
188 total nitrogen, which means that the removal of NO_3^- by Mg-Al alloy was dominated by chemical reduction.
189 The removal rate of 12% for nitrate by Mg+$AlCl_3$ (Fig. 4c) is the result of the adsorption by *in situ* LDH
190 while nitrate is not removed in the systems of Mg+Al and Mg (Fig. 4g, i). This indicates that Mg does not
191 reduce nitrate and nitrate removal by Mg-Al alloy is likely a combined effect of the chemical reduction
192 catalysed by the intermetallic compound $Mg_{17}Al_{12}$ and *in situ* LDH adsorption. The catalysis of $Mg_{17}Al_{12}$
193 on the chemical reduction of Ni(II) by Mg was reported (Chang and Uan 2021) while the mixtures of
194 $Mg_{17}Al_{12}$ and LDH were observed (Fig. 5a).

195 Fig. 6 shows the results of XPS analysis for the reaction product of Mg-Al alloy with contaminated water.
196 The peaks at 476.9 eV and 585.8 eV were assigned to Cr(III) and those at 579.3 and 588.2 eV were for
197 Cr(VI) (Tran et al. 2019). Both Cu(0) and Cu(II) were detected. Clearly, the occurrence of Cr(III) and Cu(0)
198 was the result of the chemical reduction of Cr(VI) and Cu(II), respectively. Cd, Ni and Zn were all in the
199 divalent form and they were removed from solution either in the hydroxides co-precipitates or hybrid LDH.
200 Thus, the removal of heavy metals by Mg-Al alloy involves chemical reduction, *in situ* hybrid LDH
201 adsorption/formation and hydroxide co-precipitation, depending on the nature of the heavy metal ions. For
202 example, the removal of Cu^{2+} involves the chemical reduction to Cu^0 and probably the precipitation of
203 $Cu(OH)_2$ rather than the *in situ* formation of hybrid Mg/Cu/Al-LDH because the formation of Cu-based

LDH is much more difficult due to the Jahn–Teller effect (Wu et al. 2020). The chemical reduction mechanism dominates Cu^{2+} removal because the chemical reduction still slowly proceeds at alkaline pH values. Zn^{2+} is removed most likely by the *in situ* formation of Mg/Zn/Al-LDH rather than the precipitation of $Zn(OH)_2$ because the solubility constant of the former is significantly lower than the later (1×10^{-58} *versus* 3×10^{-17}) (El-eswed 2020; Kong et al. 2020; Liu et al. 2011). The detailed mechanism of heavy metal removal by Mg-Al alloy is currently under investigation.

3.3 Effect of reaction time

The effect of reaction time on in situ LDH formation and the contaminant removal is shown in Fig. 7. The intensity of LDH's characteristic peaks increases with reaction time. This indicates that crystallinity of *in situ* LDH increases with time and at least 6 hours are required to generate enough amount of LDH that can be detected by XRD (Fig. 7a). Such slow kinetics for LDH formation may be conducive to maintain surface reactivity of Mg-Al alloy. In comparison, the formation of Fe hydroxide and oxide precipitation occur immediately when ZVI is exposed to acidic water, thus instantly passivating the surface of ZVI particles (He et al. 2006; Li et al. 2019; Theiss et al. 2016). Although the in-situ LDH formation process is relatively slow, the removal of heavy metals is swift. More than 98% of heavy metals are removed within 1 h at the rate constants of 2.2-9.2 h^{-1} (Fig. 7b). By contrast, nitrate removal is significantly slower at a rate constant of 0.2 h^{-1} (see insert of Fig. 7b).

One of the major disadvantages of ZVI and nZVI in treating contaminated, acidic water is secondary contamination by high concentrations of FeOOH, Fe_2O_3, and Fe_3O_4 (Bae et al. 2018). Therefore, Mg-Al alloy and ZVI are compared by investigating the effect of reaction time on the treatment of acidic pH 2 water contaminated by Cd, Cr(VI), Cu, Ni and Zn (Fig. 8). For Mg-Al alloy, the concentrations of heavy metals are all reduced to < 0.1 mg L^{-1} from 20 mg L^{-1} and the pH of the solution quickly rises from pH 2 to pH 8.8 in 1.5 h and then stabilizes at pH 9.0 (Fig. 8a). The quantity of LDH increases and the LDH's crystallinity is improved with reaction time (Fig. 8b). The particle size of LDH is between 450-300 nm and the concentration of Mg^{2+} and Al^{3+} ions is less than 4.0 mg L^{-1} and 0.1 mg L^{-1}, respectively (Fig. 8c). LDH sedimentation is well established (Fig. 8d). For ZVI, the removal efficiency of Cd, Cr and Ni by ZVI is much lower and the pH of the solution stabilizes at pH 4 (Fig. 8e). The resultant suspensions are FeO(OH) (JCPDS Card No. 08-0098) and Fe_3O_4 (JCPDS Card No. 19-0629) (Fig. 8f) in the particle size of around

100 nm (Fig. 8g) and the suspensions of FeO(OH) and Fe_3O_4 at high concentrations of 106-231 mg L^{-1} are not settled in 104 days (Fig. 8h), even over an extended period of 300 days. The high concentrations of iron oxide particles/colloids are the major component of acid mine drainage (AMD) and Fe is one of the most dangerous metals in AMD, which is often marked by "yellow boy", an orange-yellow substance (Rodríguez-Galán et al. 2019). AMD is a major water quality problem in the mine sites as the acidity of the water (usually the pH of AMD is typically around 3) plus the high metal concentrations can be deadly to animals and plants inhabiting the receiving streams. In this context, ZVI-based remediation technology suffers potential risks of secondary contamination with Fe.

3.4 Effect of initial pH

One of the major issues associated with AC, ZVI and pre-prepared LDH for water decontamination is their high dependence on the pH of the water (Guan et al. 2015; Jeirani et al. 2017; Zubair et al. 2017). AC and LDH are not effective to remove heavy metals, anionic and cationic dyes at pH values lower than 2 (Bhatnagar et al. 2013; Zubair et al. 2017) while the reactivity of ZVI decreases sharply with increasing pH and the surface of ZVI is rapidly passivated at pH higher than 5 (Guan et al. 2015). pH is a critical parameter affecting removal efficiency and mechanism for many pollutants. The majority of heavy metal ions are ready to precipitate in hydroxides out of aqueous solutions and/or to produce metal colloids at near neutral pH and above while organic substances are adsorbed by AC more efficiently at acidic pH than at alkaline pH. In this context, the removal of heavy metals and organic pollutants by adsorption should be performed at alkaline and acidic pH, respectively. Clearly, the removal of heavy metals by adsorption from water at alkaline pH does not fully reflect the real capability of the material. To avoid such interferences, the effect of pH was comparably investigated in this study for the removal of heavy metals at pH 3.5, methyl blue at pH 8 and glyphosate at pH 9 by Mg-Al alloy, ZVI and commercial MgAl-LDH (cLDH) (Fig. 9). Overall, Mg-Al alloy shows the best performance for heavy metals and organic pollutants within pH ranging from 3 to 9 (Fig. 9) compared to ZVI (Fig. 9b1) and cLDH (Fig. 9c1). For the Mg-Al alloy system, Mg ion concentration increases rapidly from 0 to 16 mg L^{-1} within 30 min at a rate of 31.6 mg L min^{-1} and then slows down at a rate of 1.9 mg $(L\ min)^{-1}$. In contrast, Al^{3+} concentration is less than 0.1 mg L^{-1} during the whole course of experiment. For the ZVI system, Fe ion concentration increases from 0 to 17 mg L^{-1} within 3 h and then declines sharply. This is attributed to pH increase resulting in the precipitation of iron

hydroxides (Fig. 9 b1). In the cLDH system, Mg and Al ions are gradually released reaching 6.1 mg L^{-1} and 0.6 mg L^{-1} within 3 h (Fig. 9 c1). This is the result of the dissolution of part of cLDH at initial pH 3.5.

The above results provide compelling evidence that Mg-Al alloy offer greater performance advantages for treating groundwater across a wide range of pH compared to ZVI and other systems.

3.5 Removal of multiple contaminants

Table 1 presents removal efficiencies and final concentrations of Mg, Al and Fe for a range of chemical mixtures from a synthetic groundwater sample at pH 2 by Mg-Al alloy, ZVI, AC and cLDH. The Mg-Al alloy removes ≥99.8% of each pollutant (except for glyphosate >90.0%) and the dissolved concentrations of Mg^{2+} Al^{3+} and Fe^{3+} after treatment are 56, <0.1 and <0.05 mg L^{-1}, respectively. In contrast, ZVI removes ≥ 99.8% of Zn^{2+}, AsO_3^{3-} and methyl blue, >95% of Cr(VI), Cu^{2+}, glyphosate and trichloroacetic acid, and less than 76% for Cd^{2+}, Ni^{2+} and NO_3^- . Further to this, high concentration of Fe was co-produced during the process (up to 222 mg L^{-1}) resulting in secondary pollution. AC is excellent for the removal of trichloroacetic acid and methyl blue but it shows poor performance for heavy metals, NO_3^- and glyphosate and causes a secondary contamination with Fe and Al. Despite that LDH has been reported to show excellent performance for adsorption for a wide variety of micropollutants including heavy metals, anions and organics (Theiss et al. 2014; Zubair et al. 2017), the commercial Mg/Al-LDH employed in this study is extremely poor for removing heavy metals (Cd^{2+}, Ni^{2+}, Zn^{2+}, Cu^{2+}, Cr(VI)), anions (NO_3^-, AsO_3^{3-}) and organic pollutants (methyl blue, glyphosate, trichloroacetic acid) from this particular groundwater sample.

The commercial LDH is characterized as $[Mg_6Al_2(OH)_{16}]^{2+}(CO_3)^{2-} \cdot 4H_2O$ with a BET surface area of 15.3 m^2 g^{-1}. Lin et al. (2018) observed a similar BET surface area of 18.19 m^2 g^{-1} for their laboratory-synthesized CO_3^2-LDH. The BET surface area of LDH synthesized by co-precipitation and hydrothermal precipitation was between 1.8-179 m^2 g^{-1}, depending on the conditions of the preparation (Goh et al. 2008; Tran et al. 2019). The *in situ* LDHs obtained from Mg-Al alloy are found to have BET surface areas of 27.9-31.2 m^2 g^{-1} while the BET surface area of AC employed is 1052 m^2 g^{-1}. It is considered that the superior performance of Mg-Al alloy comes from the reactivities of Mg-Al alloy and *in situ* LDH rather than the BET surface area of the material. The removal of trichloroacetic acid by ZVI and Al-Fe alloy was found through reductive dechlorination (Ding et al. 2019; Wu et al. 2019) while glyphosate and methyl blue were removed by LDH via adsorption at a capacity range of 90-384 mg g^{-1} (Feng et al. 2020; Li et al. 2020; Qiao

et al. 2018). In this context, the detailed mechanism of Mg-Al alloy for groundwater remediation warrants a further investigation.

4. Conclusions

This study demonstrates the great potential of Mg-Al alloy for the remediation of groundwater as well as the treatment of acidic wastewaters. Mg-Al alloy can be directly applied to remove a wide variety of pollutants from acidic to alkaline water without pre-dosing any other chemicals. The removal kinetics follow the pseudo-first-order of reaction and the rate constants are between 2-5 h^{-1} for 25 mg L^{-1} Cu, Zn, Ni, Cr and Cd at initial pH 2 and a dosage of 1g/100 mL. Mg-Al alloy removes ≥99% of the heavy metals, AsO_3^{3-}, nitrate, glyphosate, methyl blue and trichloroacetic acid. It outperforms ZVI and AC mainly due to a combined effect of chemical reduction and *in situ* LDH formation. Future work will need to investigate the type of pollutants, alloy's composition and durability, column studies, field testing and the detailed mechanisms of pollutant removal.

Acknowledgment

This work was supported by Ministry of Ecology and Environment (grant numbers 2018ZX07109-002) and State Administration for Market Regulation (grant numbers 21-ANL1806).

Reference

Akcil, A.,Koldas, S., 2006. Acid Mine Drainage (AMD): causes, treatment and case studies. J. Clean. Prod. 14, 1139-1145. https://doi.org/https://doi.org/10.1016/j.jclepro.2004.09.006

Ali, I.,Al-Hammadi, S.A.,Saleh, T.A., 2018. Simultaneous sorption of dyes and toxic metals from waters using synthesized titania-incorporated polyamide. J. Mol. Liq. 269, 564-571. https://doi.org/10.1016/j.molliq.2018.08.081

Bae, S.,Collins, R.N.,Waite, T.D.,Hanna, K., 2018. Advances in Surface Passivation of Nanoscale Zerovalent Iron: A Critical Review. Environ. Sci. Technol. 52, 12010-12025. https://doi.org/10.1021/acs.est.8b01734

Bao, Z.,Hu, Q.,Qi, W.,Tang, Y.,Wang, W.,Wan, P.,Chao, J.,Yang, X.J., 2017. Nitrate reduction in water by

317 aluminum alloys particles. J. Environ. Manage. 196, 666-673.
318 https://doi.org/10.1016/j.jenvman.2017.03.080
319 Bhatnagar, A.,Hogland, W.,Marques, M.,Sillanpää, M., 2013. An overview of the modification methods of
320 activated carbon for its water treatment applications. Chem. Eng. J. 219, 499-511.
321 https://doi.org/10.1016/j.cej.2012.12.038
322 Boclair, J.W.,Braterman, P.S., 1999. Layered Double Hydroxide Stability. 1. Relative Stabilities of Layered
323 Double Hydroxides and Their Simple Counterparts. Chem. Mater. 11, 298-302.
324 https://doi.org/10.1021/cm980523u
325 Bukhtiyarova, M.V., 2019. A review on effect of synthesis conditions on the formation of layered double
326 hydroxides. J. Solid State Chem. 269, 494-506. https://doi.org/10.1016/j.jssc.2018.10.018
327 Burri, N. M., 2019. A review of threats to groundwater quality in the anthropocene. Sci. Total Environ. 684, 136-
328 154 https://doi.org/10.1016/j.scitotenv.2019.05.236
329 Chang, Y.C.,Uan, J.Y., 2021. $Mg_{17}Al_{12}$ phase in magnesium alloy waste facilitating the Ni^{2+} reduction in nickel
330 plating wastewater. J. Hazard. Mater. 403, 123556. https://doi.org/10.1016/j.jhazmat.2020.123556
331 Chih-Ming K.,Yih-Terng S., Jiun-Hau O., Wei-Han L., 2020. Chapter 7 - Application of slow-release materials
332 for in situ and passive remediation of contaminated groundwater, in: Hou D., (eds), Sustainable Remediation
333 of Contaminated Soil and Groundwater. Butterworth-Heinemann, Oxford, United Kingdom, pp. 169-199.
334 https://doi.org/10.1016/B978-0-12-817982-6.00007-0
335 Cohen, M.,Weisbrod, N., 2018. Field Scale Mobility and Transport Manipulation of Carbon-Supported
336 Nanoscale Zerovalent Iron in Fractured Media. Environ. Sci. Technol. 52, 7849-7858.
337 https://doi.org/10.1021/acs.est.8b01226
338 Ding, S.,Deng, Y.,Bond, T.,Fang, C.,Cao, Z.,Chu, W., 2019. Disinfection byproduct formation during drinking

water treatment and distribution: A review of unintended effects of engineering agents and materials. Water Res. 160, 313-329. https://doi.org/10.1016/j.watres.2019.05.024

Douglas, G.,Shackleton, M.,Woods, P., 2014. Hydrotalcite formation facilitates effective contaminant and radionuclide removal from acidic uranium mine barren lixiviant. Appl. Geochem. 42, 27-37. https://doi.org/10.1016/j.apgeochem.2013.12.018

El-eswed, B.I., 2020. Chemical evaluation of immobilization of wastes containing Pb, Cd, Cu and Zn in alkali-activated materials: A critical review. J. Environ. Chem. Eng. 8, 104194. https://doi.org/10.1016/j.jece.2020.104194

Feng, D.,Soric, A.,Boutin, O., 2020. Treatment technologies and degradation pathways of glyphosate: A critical review. Sci. Total Environ. 742, 140559. https://doi.org/10.1016/j.scitotenv.2020.140559

Fu, F.,Cheng, Z.,Dionysiou, D.D.,Tang, B., 2015. Fe/Al bimetallic particles for the fast and highly efficient removal of Cr(VI) over a wide pH range: Performance and mechanism. J. Hazard. Mater. 298, 261-269. https://doi.org/10.1016/j.jhazmat.2015.05.047

Fu, F.,Dionysiou, D.D.,Liu, H., 2014. The use of zero-valent iron for groundwater remediation and wastewater treatment: a review. J. Hazard. Mater. 267, 194-205. https://doi.org/10.1016/j.jhazmat.2013.12.062

Goh, K.H.,Lim, T.T.,Dong, Z., 2008. Application of layered double hydroxides for removal of oxyanions: a review. Water Res. 42, 1343-1368. https://doi.org/10.1016/j.watres.2007.10.043

Guan, X.,Sun, Y.,Qin, H.,Li, J.,Lo, I.M.C.,He, D.,Dong, H., 2015. The limitations of applying zero-valent iron technology in contaminants sequestration and the corresponding countermeasures: The development in zero-valent iron technology in the last two decades (1994–2014). Water Res. 75, 224-248. https://doi.org/10.1016/j.watres.2015.02.034

Guo, L.,Wu, W.,Zhou, Y.,Zhang, F.,Zeng, R.,Zeng, J., 2018. Layered double hydroxide coatings on magnesium

alloys: A review. J. Mater. Sci. Technol. 34, 1455-1466. https://doi.org/10.1016/j.jmst.2018.03.003

He, J.,Wei, M.,Li, B.,Kang, Y.,Evans, D.G.,Duan, X. 2006. Preparation of Layered Double Hydroxides, in: Duan X., Evans D.G., (eds), Layered Double Hydroxides. Springer Berlin Heidelberg, Berlin, Heidelberg, pp. 89-119. https://doi.org/10.1007/430_006

He, X.,Qiu, X.,Hu, C.,Liu, Y., 2017. Treatment of heavy metal ions in wastewater using layered double hydroxides: A review. J. Disper. Sci. Technol. 39, 792-801. https://doi.org/10.1080/01932691.2017.1392318

Jeirani, Z.,Niu, C.H.,Soltan, J., 2017. Adsorption of emerging pollutants on activated carbon. Rev. Chem. Eng. 33, 491-522. https://doi.org/10.1515/revce-2016-0027

Kong, X.,Ge, R.,Liu, T.,Xu, S.,Hao, P.,Zhao, X.,Li, Z.,Lei, X.,Duan, H., 2020. Super-stable mineralization of cadmium by calcium-aluminum layered double hydroxide and its large-scale application in agriculture soil remediation. Chem. Eng. J. 407, 127178. https://doi.org/10.1016/j.cej.2020.127178

Lei, L., Song, C., Xie X., Li, Y., 2008. REE behavior and effect factors in AMD-type acidic groundwater at sulfide tailings pond, BS nickel mine, W.A. Trans. Nonferrous Met. Soc. China 18, 955-961. https://doi.org/10.1016/S1003-6326(08)60165-X

Lei, L., Song, C., Xie X., Li, Y., Wang, F., 2008. Acid mine drainage and heavy metal contamination in groundwater of metal sulfide mine at arid territory (BS mine, Western Australia). Trans. Nonferrous Met. Soc. China 20, 1488-1493. https://doi.org/10.1016/S1003-6326(09)60326-5

Li, G.,Zhang, X.,Sun, J.,Zhang, A.,Liao, C., 2020. Effective removal of bisphenols from aqueous solution with magnetic hierarchical rattle-like Co/Ni-based LDH. J. Hazard. Mater. 381, 120985. https://doi.org/10.1016/j.jhazmat.2019.120985

Li, J.,Dou, X.,Qin, H.,Sun, Y.,Yin, D.,Guan, X., 2019. Characterization methods of zerovalent iron for water treatment and remediation. Water Res. 148, 70-85. https://doi.org/10.1016/j.watres.2018.10.025

Lin, S.T.,Tran, H.N.,Chao, H.P.,Lee, J.F., 2018. Layered double hydroxides intercalated with sulfur-containing organic solutes for efficient removal of cationic and oxyanionic metal ions. Appl. Clay Sci. 162, 443-453. https://doi.org/10.1016/j.clay.2018.06.011

Liu, Q.,Li, Y.,Zhang, J.,Chi, Y.,Ruan, X.,Liu, J.,Qian, G., 2011. Effective removal of zinc from aqueous solution by hydrocalumite. Chem. Eng. J. 175, 33-38. https://doi.org/10.1016/j.cej.2011.09.022

Ma, L.,Islam, S.M.,Liu, H.,Zhao, J.,Sun, G.,Li, H.,Ma, S.,Kanatzidis, M.G., 2017. Selective and Efficient Removal of Toxic Oxoanions of As(III), As(V), and Cr(VI) by Layered Double Hydroxide Intercalated with MoS_4^{2-}. Chem. Mater. 29, 3274-3284. https://doi.org/10.1021/acs.chemmater.7b00618

Nguyen, N.H.A.,Von Moos, N.R.,Slaveykova, V.I.,Mackenzie, K.,Meckenstock, R.U.,Thűmmler, S.,Bosch, J.,Ševců, A., 2018. Biological effects of four iron-containing nanoremediation materials on the green alga Chlamydomonas sp. Ecotoxicol. Environ. Saf. 154, 36-44. https://doi.org/10.1016/j.ecoenv.2018.02.027

Nidheesh, P.V.,Khatri, J.,Anantha Singh, T.S.,Gandhimathi, R.,Ramesh, S.T., 2018. Review of zero-valent aluminium based water and wastewater treatment methods. Chemosphere 200, 621-631. https://doi.org/https://doi.org/10.1016/j.chemosphere.2018.02.155

Oestreicher, V.,Fábregas, I.,Jobbágy, M., 2014. One-Pot Epoxide-Driven Synthesis of M2Al(OH)6Cl·1.5H2O Layered Double Hydroxides: Precipitation Mechanism and Relative Stabilities. The Journal of Physical Chemistry C 118, 30274-30281. https://doi.org/10.1021/jp510341q

Qiao, Y.,Li, Q.,Chi, H.,Li, M.,Lv, Y.,Feng, S.,Zhu, R.,Li, K., 2018. Methyl blue adsorption properties and bacteriostatic activities of Mg-Al layer oxides via a facile preparation method. Appl. Clay Sci. 163, 119-128. https://doi.org/10.1016/j.clay.2018.07.018

Rodríguez-Galán, M.,Baena-Moreno, F.M.,Vázquez, S.,Arroyo-Torralvo, F.,Vilches, L.F.,Zhang, Z., 2019. Remediation of acid mine drainage. Environ. Chem. Lett. 17, 1529-1538. https://doi.org/10.1007/s10311-

019-00894-w

Saleh, T.A., 2020a. Characterization, determination and elimination technologies for sulfur from petroleum: Toward cleaner fuel and a safe environment. Trends Environ. Anal. Chem. 25, e00080. https://doi.org/https://doi.org/10.1016/j.teac.2020.e00080

Saleh, T.A., 2020b. Nanomaterials: Classification, properties, and environmental toxicities. Environ. Technol. Inno. 20, 101067. https://doi.org/10.1016/j.eti.2020.101067

Saleh, T.A., 2020c. Trends in the sample preparation and analysis of nanomaterials as environmental contaminants. Trends Environ. Anal. Chem. 28, e00101. https://doi.org/10.1016/j.teac.2020.e00101

Scaria, J.,Nidheesh, P.V.,Kumar, M.S., 2020. Synthesis and applications of various bimetallic nanomaterials in water and wastewater treatment. J. Environ. Manage. 259, 110011. https://doi.org/10.1016/j.jenvman.2019.110011

Schwarzenbach, R.P.,Escher, B.I.,Kathrin, F.,Hofstetter, T.B.,C Annette, J.,Urs, V.G.,Bernhard, W., 2006. The challenge of micropollutants in aquatic systems. Science 313, 1072-1077. https://doi.org/10.1126/science.1127291

Shannon, M.A.,Bohn, P.W.,Elimelech, M.,Georgiadis, J.G.,Mariñas, B.J.,Mayes, A.M., 2008. Science and technology for water purification in the coming decades. Nature 452, 301-310. https://doi.org/10.1038/nature06599

Shukla, N.,Saxena, A.,Gupta, V.,Rawat, A.S.,Shrivastava, S.,Rai, P.K., 2018. Nano Zero Valent Iron Composites for Water Decontamination: A Review. Curr. Environ. Eng. 5, 88-101. https://doi.org/10.2174/2212717805666180405123523

Theiss, F.L.,Ayoko, G.A.,Frost, R.L., 2016. Synthesis of layered double hydroxides containing Mg^{2+}, Zn^{2+}, Ca^{2+} and Al^{3+} layer cations by co-precipitation methods—A review. Appl. Surf. Sci. 383, 200-213.

https://doi.org/10.1016/j.apsusc.2016.04.150

Theiss, F.L.,Couperthwaite, S.J.,Ayoko, G.A.,Frost, R.L., 2014. A review of the removal of anions and oxyanions of the halogen elements from aqueous solution by layered double hydroxides. J. Colloid Interface Sci. 417, 356-368. https://doi.org/10.1016/j.jcis.2013.11.040

Tosco, T.,Petrangeli Papini, M.,Cruz Viggi, C.,Sethi, R., 2014. Nanoscale zerovalent iron particles for groundwater remediation: a review. J. Clean. Prod. 77, 10-21. https://doi.org/10.1016/j.jclepro.2013.12.026

Tran, H.N.,Nguyen, D.T.,Le, G.T.,Tomul, F.,Lima, E.C.,Woo, S.H.,Sarmah, A.K.,Nguyen, H.Q.,Nguyen, P.T.,Nguyen, D.D.,Nguyen, T.V.,Vigneswaran, S.,Vo, D.N.,Chao, H.P., 2019. Adsorption mechanism of hexavalent chromium onto layered double hydroxides-based adsorbents: A systematic in-depth review. J. Hazard. Mater. 373, 258-270. https://doi.org/10.1016/j.jhazmat.2019.03.018

Tran, H.N.,You, S.J.,Hosseini-Bandegharaei, A.,Chao, H.P., 2017. Mistakes and inconsistencies regarding adsorption of contaminants from aqueous solutions: A critical review. Water Res. 120, 88-116. https://doi.org/10.1016/j.watres.2017.04.014

Wang, S.,Song, Y.,Sun, Y., 2019. Performance and Mechanism of Contaminants Removal by Carbon Materials Modified Zerovalent Iron. Prog. Chem. 31, 422-432. https://doi.org/10.7536/PC180726

Wu, L.,Peng, B.,Li, Q.,Wang, Q.,Yan, X.,Li, K.,Lin, Q., 2020. Effects of Cu^{2+} incorporation on ZnAl-layered double hydroxide. New J. Chem. 44, 5293-5302. https://doi.org/10.1039/D0NJ00278J

Wu, S.,Tang, K.,Zhang, J.,Chen, X.,Hu, H.,Hu, Q.,Yang, X.J., 2019. Removal of 4-chlorophenol from polluted water by aluminum-iron alloys. Water Sci. Technol. 80, 1099-1106. https://doi.org/10.2166/wst.2019.349

Xu, J.,Pu, Y.,Yang, X.J.,Wan, P.,Wang, R.,Song, P.,Fisher, A., 2018. Rapid removal of chloroform, carbon tetrachloride and trichloroethylene in water by aluminum-iron alloy particles. Environ. Technol. 39, 2882-2890. https://doi.org/10.1080/09593330.2017.1369577

449 Xu, L.,Huang, Y., 2019. A novel layered double hydroxide coupled with zero valent iron system for selenate
450 removal under anaerobic condition: Batch and continuous studies. Chem. Eng. J. 359, 1166-1174.
451 https://doi.org/10.1016/j.cej.2018.11.061
452 Yang, Z.,Wang, F.,Zhang, C.,Zeng, G.,Tan, X.,Yu, Z.,Zhong, Y.,Wang, H.,Cui, F., 2016. Utilization of LDH-based
453 materials as potential adsorbents and photocatalysts for the decontamination of dyes wastewater: a review.
454 RSC Adv. 6, 79415-79436. https://doi.org/10.1039/c6ra12727d
455 Yu, S.,Wang, X.,Liu, Y.,Chen, Z.,Wu, Y.,Liu, Y.,Pang, H.,Song, G.,Chen, J.,Wang, X., 2019. Efficient removal of
456 uranium(VI) by layered double hydroxides supported nanoscale zero-valent iron: A combined experimental
457 and spectroscopic studies. Chem. Eng. J. 365, 51-59. https://doi.org/10.1016/j.cej.2019.02.024
458 Zhang, J.,Wu, J.,Chao, J.,Shi, N.,Li, H.,Hu, Q.,Yang, X.J., 2019. Simultaneous removal of nitrate, copper and
459 hexavalent chromium from water by aluminum-iron alloy particles. J. Contam. Hydrol., 103541.
460 https://doi.org/10.1016/j.jconhyd.2019.103541
461 Zheng, T.,Zhang, J.,Tang, Y.,Wan, P.,Yuan, Q.,Hu, H.,Coulon, F.,Hu, Q.,Yang, X.J., 2021. Production of High-
462 Purity Hydrogen and Layered Doubled Hydroxide by Hydrolysis of Mg-Al Alloys. Chem. Eng. Technol. 44,
463 797-803. https://doi.org/https://doi.org/10.1002/ceat.202000590
464 Zhou, M.,Zhang, C.,Yuan, Y.,Mao, X.,Li, Y.,Wang, N.,Wang, S.,Wang, X., 2020. Pinewood outperformed
465 bamboo as feedstock to prepare biochar-supported zero-valent iron for Cr^{6+} reduction. Environ. Res. 187,
466 109695. https://doi.org/10.1016/j.envres.2020.109695
467 Zubair, M.,Daud, M.,McKay, G.,Shehzad, F.,Al-Harthi, M.A., 2017. Recent progress in layered double
468 hydroxides (LDH)-containing hybrids as adsorbents for water remediation. Appl. Clay Sci. 143, 279-292.
469 https://doi.org/10.1016/j.clay.2017.04.002
470

Table 1. Removal efficiency of multiple pollutants from synthetic, polluted groundwater and released Mg, Al and Fe concentrations [a]

Pollutants	Initial conc.	Removal efficiency (%)			
	(mg L^{-1})	Mg-Al alloy	ZVI	AC	cLDH
Cd	20.2	>99.9	75.7	0.673	1.18
Cr(VI)	19.5	>99.8	97.5	15.5	10.7
Cu	20.9	>99.8	99.3	7.26	5.65
Ni	9.19	>99.8	66.5	0.102	1.39
Zn	10.4	>99.8	>99.8	0.130	1.58
AsO_3^{3-}	19.9	>99.8	>99.8	8.35	27.8
NO_3^-	53.3	>99.8	56.9	51.2	0.463
Glyphosate	19.9	>99.0	>99.0	30.7	53.1
Methyl Blue	32.4	>99.8	>99.8	>99.8	66.7
Trichloroacetic acid	20.5	>99.8	97.9	>99.8	17.1
	Metal concentration (mg L^{-1})				
Mg	21.4	56.2	17.8	23.1	102
Al	<0.100	<0.100	<0.100	2.40	42.0
Fe	<0.0500	<0.0500	222	3.34	<0.0500

[a] The contaminated water sample was prepared by dissolving $K_2Cr_2O_7$, nitrate salts and other pollutants in real groundwater samples (pH 7.87) and adjusting to pH 2 using HCl. The groundwater sample contained 4.85 mg L^{-1} K, 6.53 mg L^{-1} Na, 21.4 mg L^{-1} Mg and 61.4 mg L^{-1} Ca. The dosage of each material was 1 g 100 mL^{-1}, treatment time 9 h, treatment temperature 22 ˚C±2 □. The result is an average of three independent experiments. AC: activated carbon, ZVI: zerovalent iron, cLDH: commercial MgAl-LDH.

Journal Pre-proof

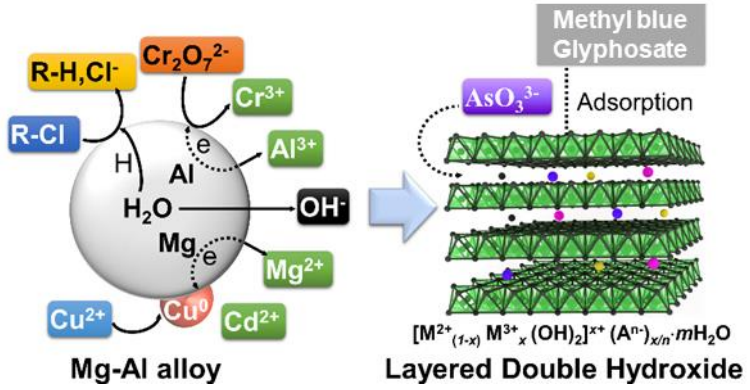


Fig. 1 Schematic illustration of model pollutants removal by Mg-Al alloy in situ layered double hydroxide from contaminated water.

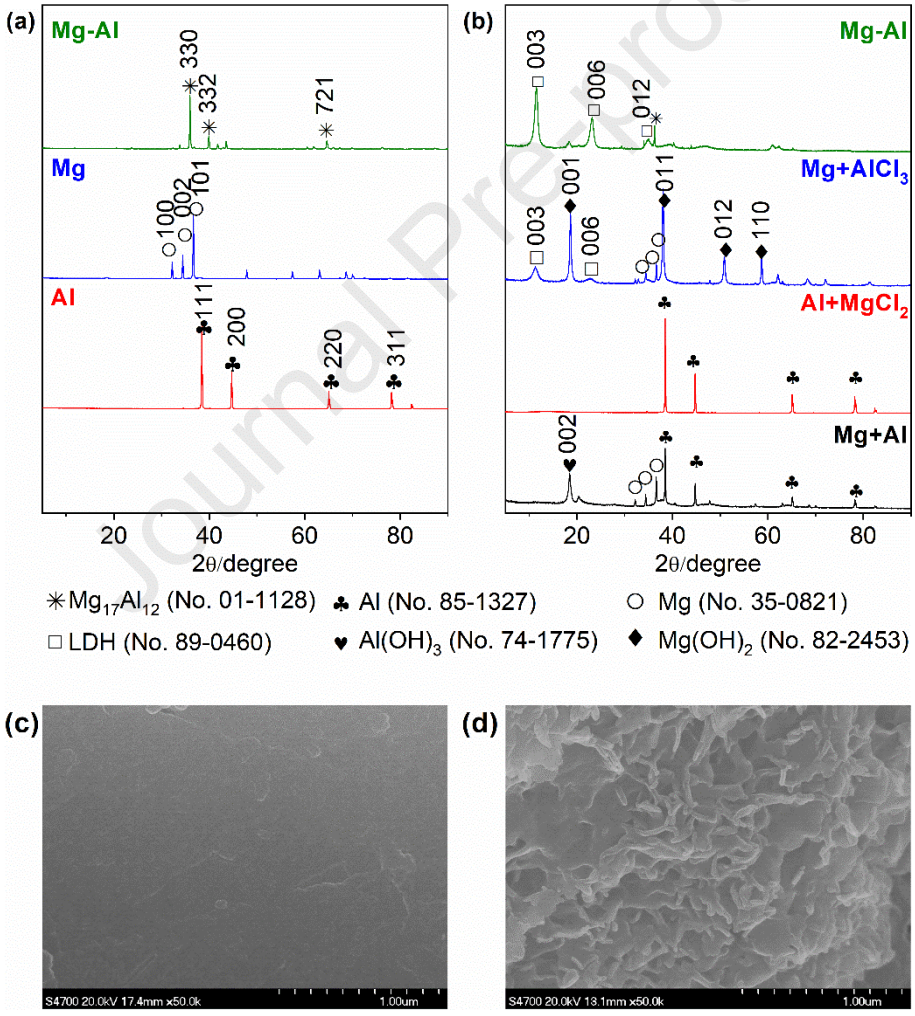


Fig. 2. (a, b) XRD and (c, d) SEM characterization. (a) Mg and Al metals and Mg-Al alloy, (b) the hydrolysis products of Mg-Al alloy, Mg+$AlCl_3$, Al+$MgCl_2$ and Mg+Al at initial pH 2 (HCl), (c) Mg-Al alloy, (d) the hydrolysis product of Mg-Al alloy. 3 g Mg-Al alloy (Mg/Al = 60/40), particle size >200 meshes; 3 g Mg metal powders (>240 meshes) in $AlCl_3$ solution (100 mg L^{-1} Al^{3+}), 3 g Al metal powders (>325 meshes) in $MgCl_2$ solution (200 mg L^{-1} Mg^{2+}), 1.8 g Mg metal powders and 1.2 g Al metal powders. Aqueous solution volume 300 mL, made to pH 2 (HCl), hydrolysis time 24 h, stirring speed of magnetic bar 300 rpm, temperature 22 °C±2 □.

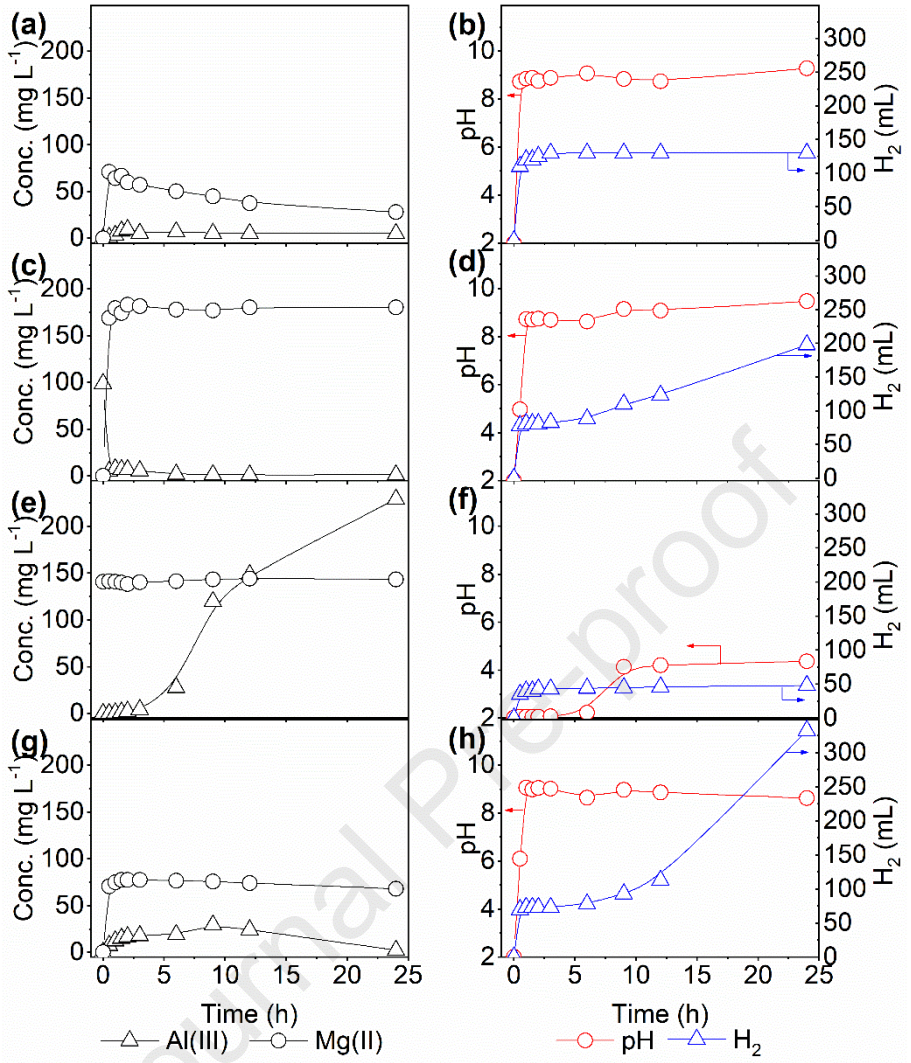


Fig. 3. Mg and Al ion concentration, pH and hydrogen generation in the experiment of Fig. 2. (a, b) Mg-Al alloy, (c, d) Mg+$AlCl_3$, (e, f) Al+$MgCl_2$ and (g, h) Mg+Al

Journal Pre-proof

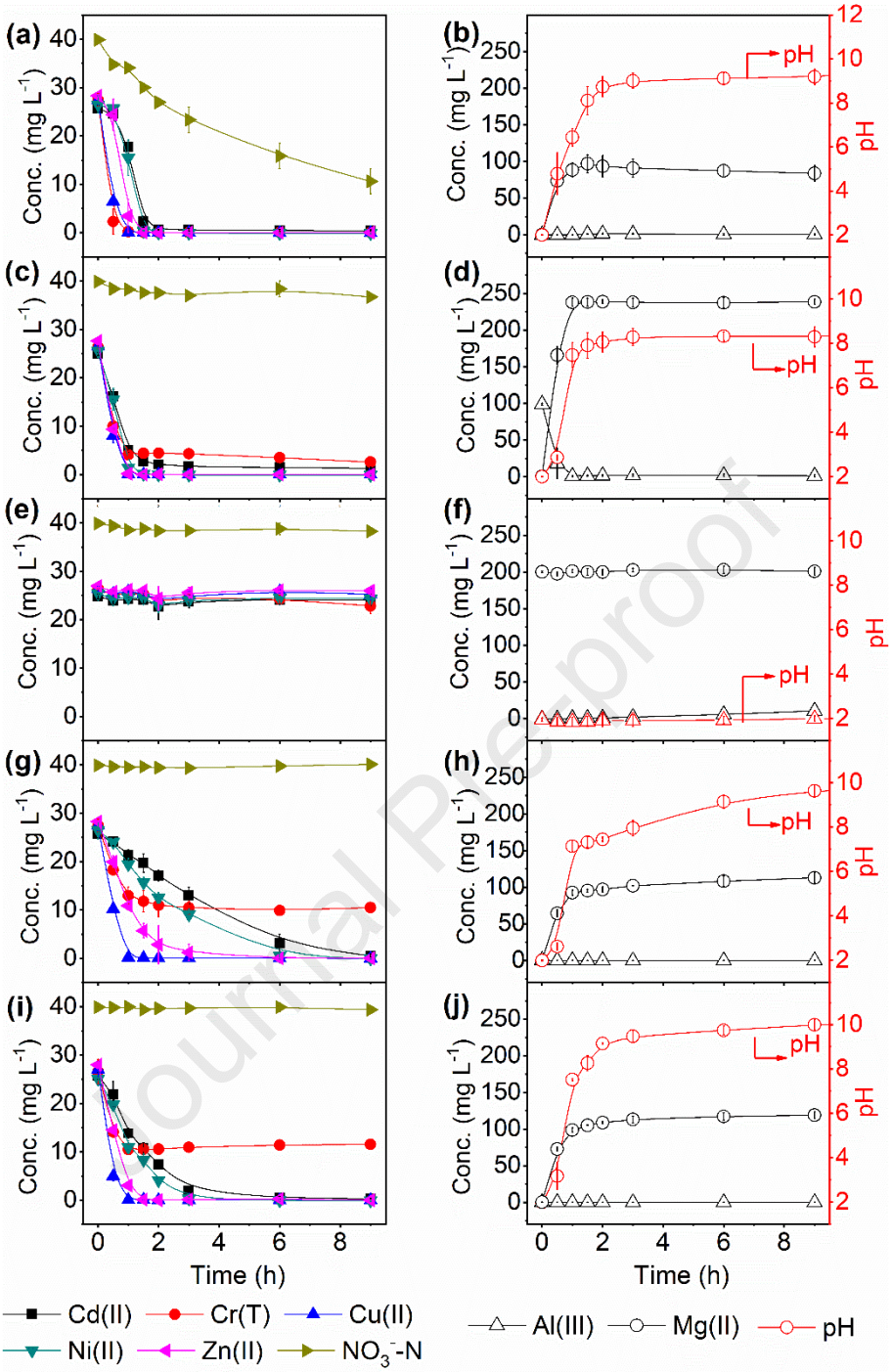


Fig. 4. Concentrations of heavy metals, nitrate, Mg and Al ions and the pH of solution as a function of reaction time in contaminated water (300 mL, pH 2). (a, b) Mg-Al alloy, (c, d) Mg+$AlCl_3$, (e, f) Al+$MgCl_2$, (g, h) Mg+Al, (i, j) Mg. Stirring speed 300 rpm, temperature 22 °C±2 □, concentration of individual heavy metal 25 mg L^{-1}, nitrate 40 mg L^{-1}, other experimental condition is the same as Fig. 2. The results are the average of three independent experiments with the standard deviation as the error bar.

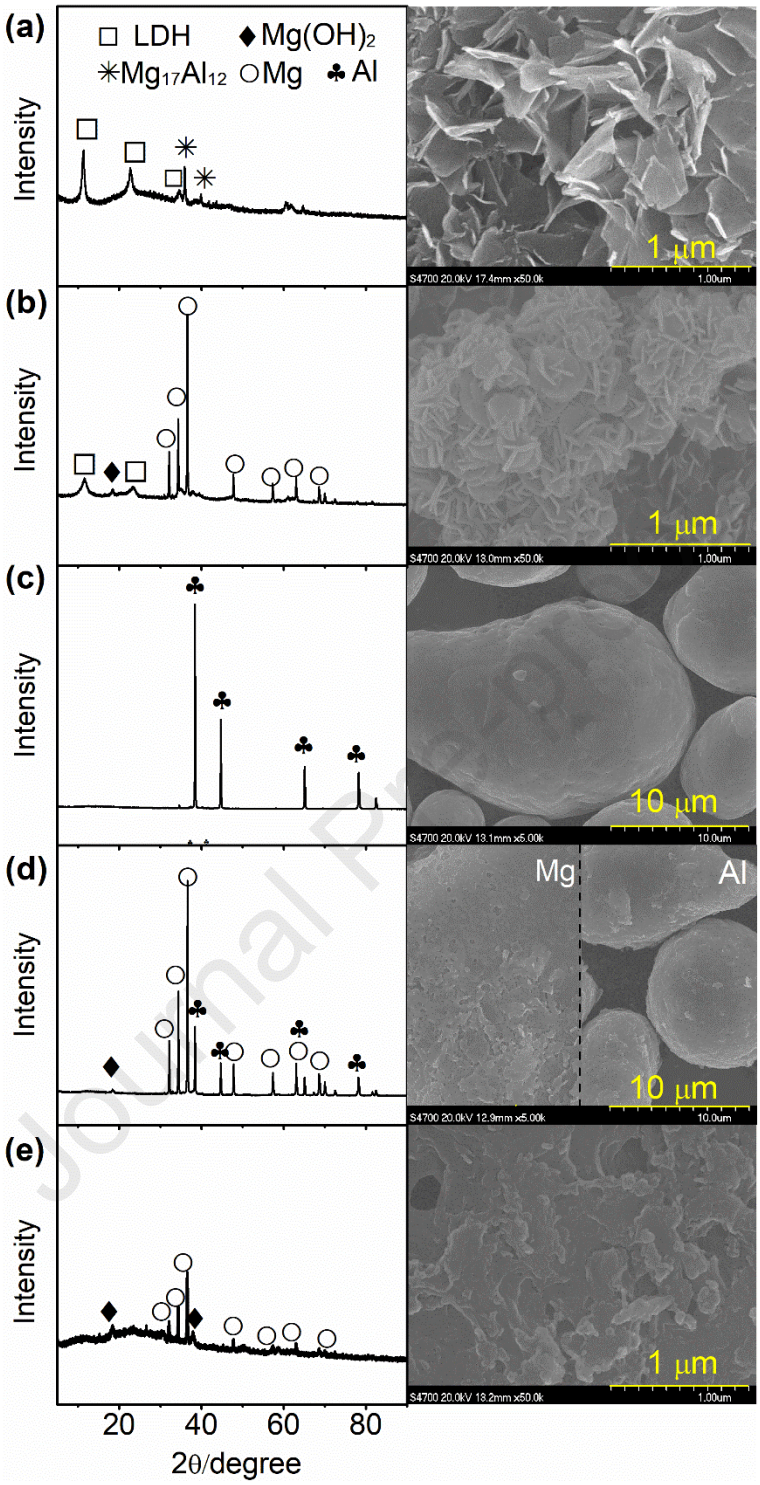


Fig. 5. XRD and SEM characterization of the materials after reaction with contaminated water as in Fig. 4. (a) Mg-Al alloy, (b) Mg+$AlCl_3$, (c) Al+$MgCl_2$, (d) Mg+Al, (e) Mg.

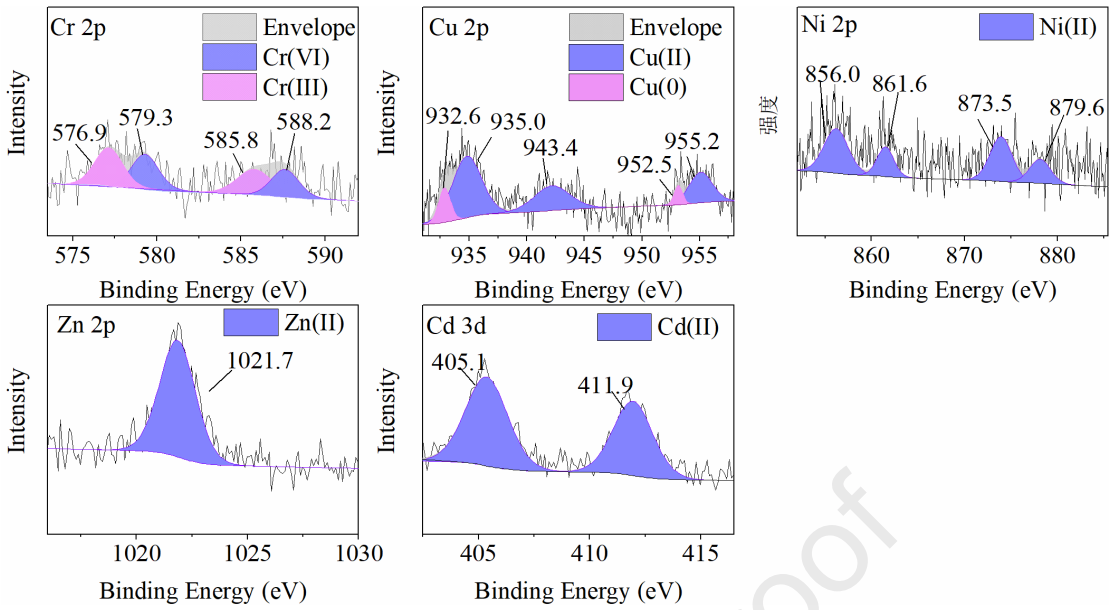


Fig. 6 XPS characterization of the reaction products of Mg-Al alloy with contaminated water. Contaminated water 300 mL, Mg-Al alloy 3 g, stirring speed 300 rpm, temperature 22±2 °C.

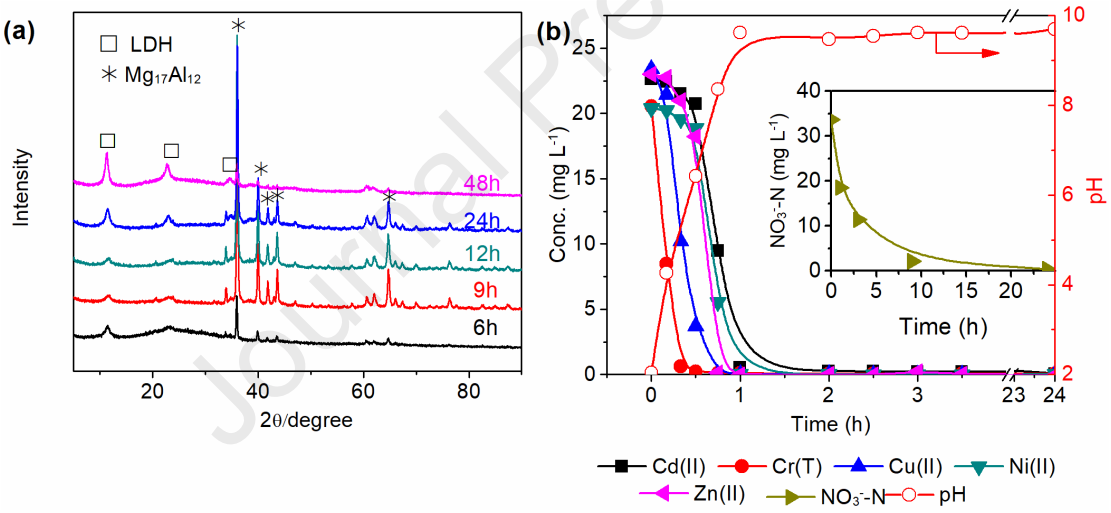


Fig. 7. Effect of reaction time on hydrolysis products and heavy metals and nitrate concentration for Mg-Al alloy and contaminated water. (a) XRD characterization of reaction products, (b) heavy metals and NO_3^- concentration and pH variation. Mg-Al alloy 3 g, contaminated water 300 mL, initial pH = 2, stirring speed 300 rpm, temperature 22 ˚C±2 □.

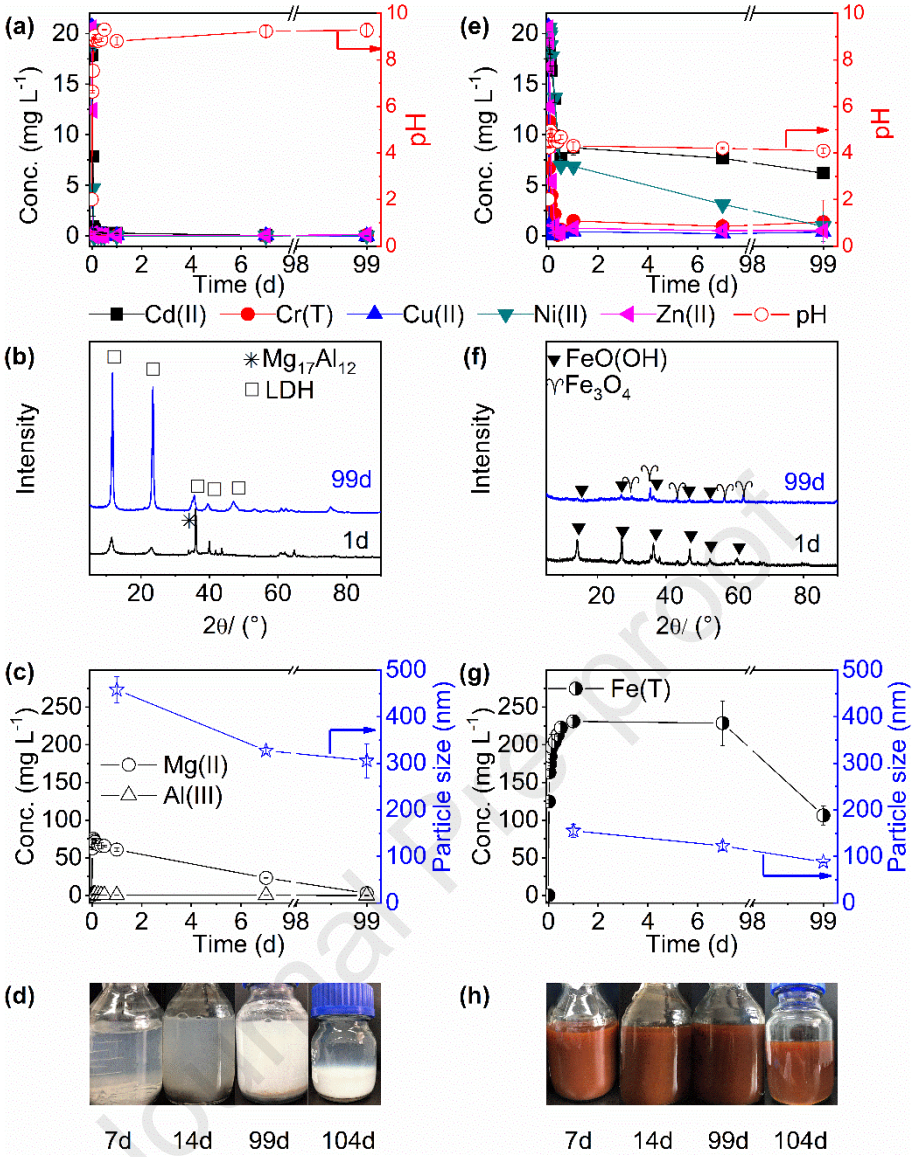


Fig. 8. Effect of reaction time on heavy metals, Al, Mg and Fe concentrations, pH and the particle size and settlement of the hydrolysis products. (a-d) Mg-Al alloy, (e-h) ZVI. Mg-Al alloy (>200 meshes, 3 g), ZVI (100-120 meshes, 3 g), contaminated water 300 mL pH 2 (HCl). The system was stirred at 300 rpm for 12 h and then stood without stirring for 99 days. Then, the suspensions were decanted to a new bottle and stood for additional 15 days. Temperature was 22 ˚C±2 □.

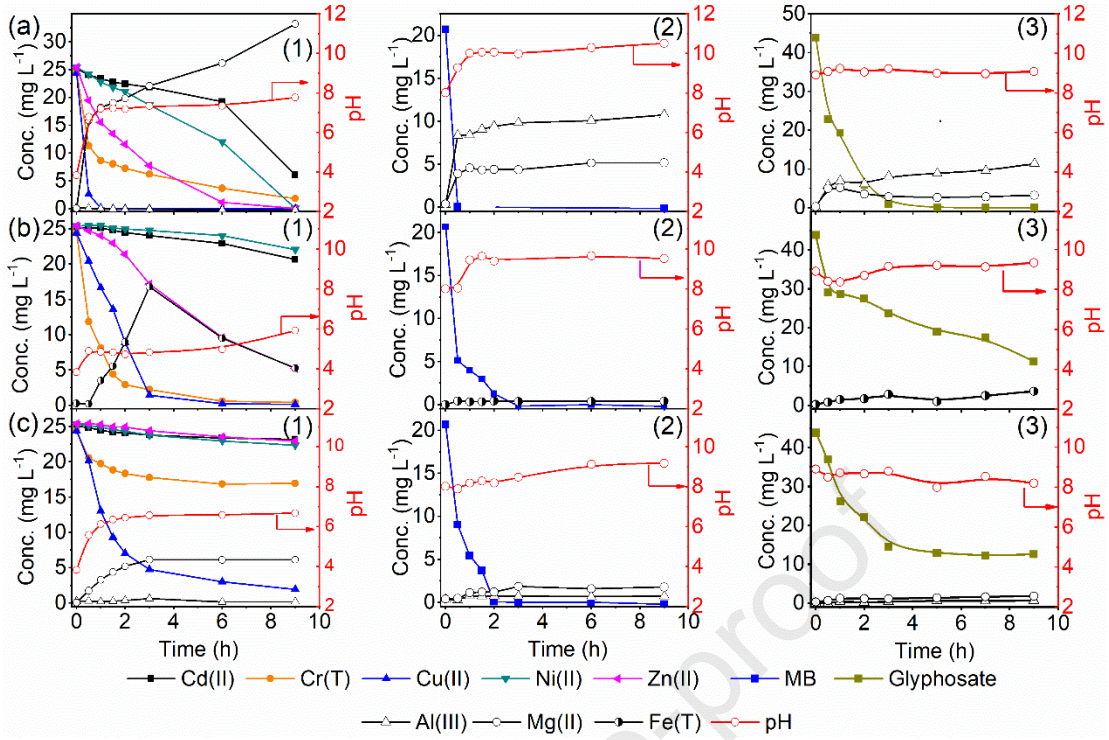


Fig. 9. Concentrations of pollutants (heavy metals, methyl blue and glyphosate), leached concentrations of Mg, Al and Fe ions, and pH variations at initial pH 3.5 (left panel), pH 8.0 (middle) and 9.0 (right). (a) Mg-Al alloy, (b) ZVI, (c) LDH. Materials 3 g, contaminated water 300 mL, reaction time 9 h, stirring speed 300 rpm, temperature 22 ˚C±2 □.

Journal Pre-proof

Journal Pre-proof

Declaration of interests

☒ The authors declare that they have no known competing financial interests or personal relationships that could have appeared to influence the work reported in this paper.

☐The authors declare the following financial interests/personal relationships which may be considered as potential competing interests:

Journal Pre-proof



https://dspace.org/

Groundwater remediation using Magnesium–Aluminum alloys and in situ layered doubled hydroxides

Zhang, Jingqi; Hu, Hanjun; Chao, Jingbo; Tang, Yang; Wan, Pingyu ...

2021-10-22
Elsevier
https://doi.org/10.1016/j.envres.2021.112241
Zhang J, Hu H, Chao J, et al., (2022) Groundwater remediation using Magnesium–Aluminum alloys and in situ layered doubled hydroxides. Environmental Research, Volume 204, Part C, March 2022, Article number 112241

Downloaded from a DSpace repository. https://dspace.org/